Neutron Production from Thin Target of Carbon and Iron by 70 MeV Protons

Toshiro Itoga, Masayuki Hagiwara, Takeshi Yamauchi, Takuji Oishi and Mamoru Baba

Cyclotron and Radioisotope Center (CYRIC), Tohoku University
6-3, Aoba, Aramaki, Aoba-ku, Sendai-shi, Miyagi-ken 980-8578
itogat@cyric.tohoku.ac.jp

Double differential neutron production cross section were measured at 70 MeV for the C, Fe(p, xn) reactions at four laboratory angles between 0- and 90-deg using the time-of-flight (TOF) method at the Tohoku University K = 110-MeV AVF cyclotron with a beam-swinger system and a low background TOF line. We determined neutron energy spectra from ~0.6 MeV to the highest secondary neutron energy. The experimental results were compared with the LA150 data library, and showed fairly good agreement/ or marked discrepancy.

1. Introduction

By the development of accelerator technology, accelerators become very reliable and high intensity and high energy accelerators are now available. Accordingly, uses of the accelerators are expanding to material studies, medical treatment, radiobiology studies and environmental science as well as nuclear physics, and some accelerators with high energy and intensity are under construction or in plan e.g., Japan Proton Accelerator Research Complex (JPARC, which is promoted by the corporation of JAERI and KEK) and Spallation Neutron Source (SNS, United States).

For the design of accelerator shielding and the accelerator-based neutron sources, differential thick target neutron yields (TTY) data are required over a wide energy and angle range with sufficiently good energy resolution. However, existing nuclear data files are not examined in quality for high energy accelerator application, and experimental data covering wide range of secondary neutron energies are very few. We have been conducting TTY measurements for proton of tens of MeV regions for the various elements shown in table 1, which are typical elements for beam-lines and beam-dumps in accelerators using a time-of-flight (TOF) method at the Cyclotron and Radioisotope Center (CYRIC), Tohoku University equipped with a K=110 AVF cyclotron and a beam-swinger system and low background TOF flight path.

These data were compared with the LA150 data library. LA150 data reproduced experimental data generally well but still shows marked disagreement in some energy and/or angular regions [1] Therefore, in the present experiment, to know the reasons of these disagreements, we measured the neutron yields for (p, xn) reactions for thin targets of carbon and iron.

Table 1: Series of TTY measurements for (p ,xn) reaction at CYRIC [1].

Energy [MeV]	Nuclide	Angle [deg.]
35	Fe, Cu	0, 30, 60, 90, 110
50	C, Al, Fe, Cu, Ta, W	0, 30, 60, 90, 110
70	C, Al, Fe, Cu, W, Pb	0, 30, 60, 90, 110

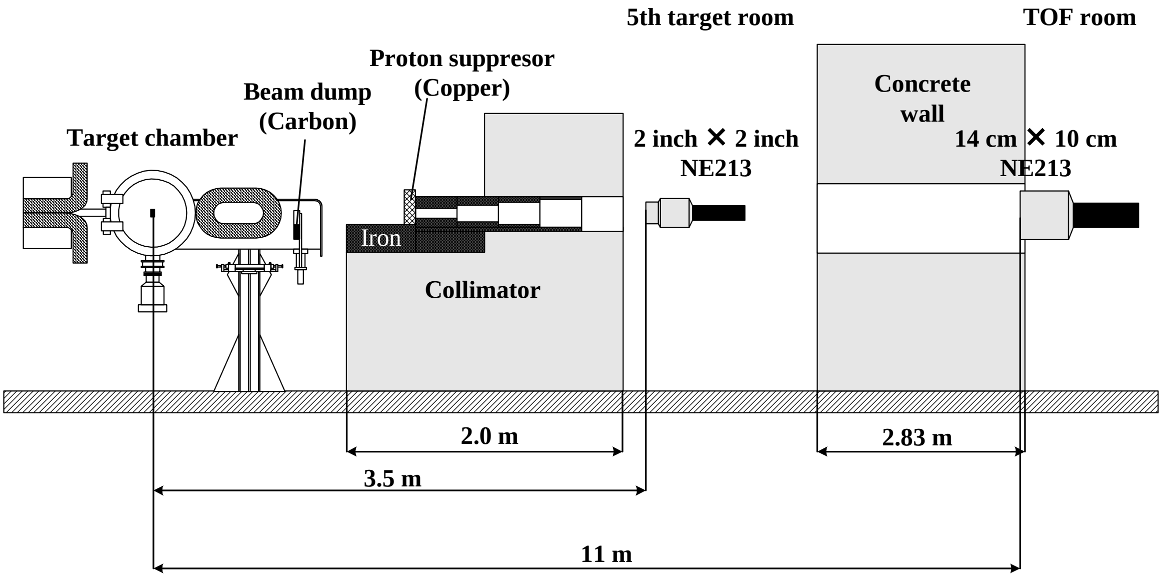

Fig. 1. Experimental setup

2. Experiment

The experimental setup is shown in fig. 1. A proton beam accelerated by the AVF cyclotron was transported to the target room No.5 of CYRIC equipped with a beam-swinger system and a neutron TOF channel [2]. The beam swinger system changes the incident angle of the beam onto the target from 0-deg to 120-deg and enables to measure angular distributions with a fixed detector setup. The targets of carbon and iron were plate of natural elements with sizes shown in table 2. After penetrating the target, a proton beam is bent to the beam dump made of carbon. The target chamber was shielded with a 2.5 m thick concrete wall having a beam channel for collimators to enable measurement of neutrons under a low background environment. In addition, to prevent the detection of neutral hydrogens, a copper plate is placed between the targets and detectors. Emitted neutrons were detected by an NE213 liquid scintillation detector, 14 cm-diam. × 10 cm-thick or 5 cm-diam × 5 cm-thick equipped with a pulse-shape-discriminator (PSD). The larger and smaller detectors were placed around ~11 m and ~3.5 m from the target, respectively. The measurement with a shorter flight path was adopted to obtain the low energy part (~0.6-4 MeV) of the neutron spectrum with low pulse-height bias, and that with a longer flight path was for higher energy part. The TOF, PSD and pulse-height data were collected event by event as three parameter list data for off-line analysis [3] together with the beam current at the beam dump concurrently.

Table 2: Target dimension

Nuclide	Thickness [mm]	Density [g/cm3]	Energy loss [%]
C	1	1.8712	2.15
Fe	0.3	8.058	2.25

3. Experimental procedures

The pulse width of proton beam was generally less than 2 ns in FWHM, and the beam interval was 492 ns by using the beam chopper to avoid frame overlap in the TOF spectra. The incident beam current on the beam dump was around 1 ~ 10 nA and was digitized and recorded by a scalar for normalization of the neutron TOF spectrum. The TOF data were obtained at four laboratory angles (0, 30, 60 and 90 deg.).

4. Data analysis

Neutron TOF spectra gated by the PSD signal and the lower pulse-height bias were converted into energy spectra after subtraction with flat background components. The efficiency vs. energy curves of the detectors were obtained by the calculation with a SCINFUL-R, which is revised version of the Monte Carlo code SCINFUL [4] and was verified to be accurate within ± 5 % up to 80 MeV [5]. Then the data have been corrected for the effect of neutron attenuation in the target, air, and the copper proton stopper using the ENDF/B-VI evaluated neutron data library. Finally, two neutron energy spectra obtained by two detectors were normalized with the integrated beam current and connected at 4 MeV to deduce whole energy spectrum.

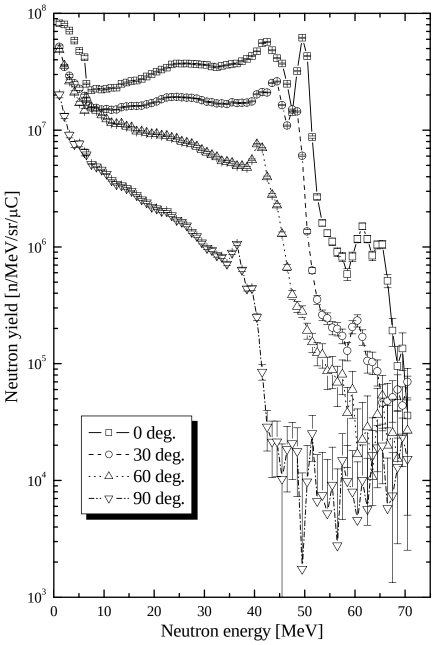

Fig. 2. ^{nat}C(p, xn) neutron production cross section

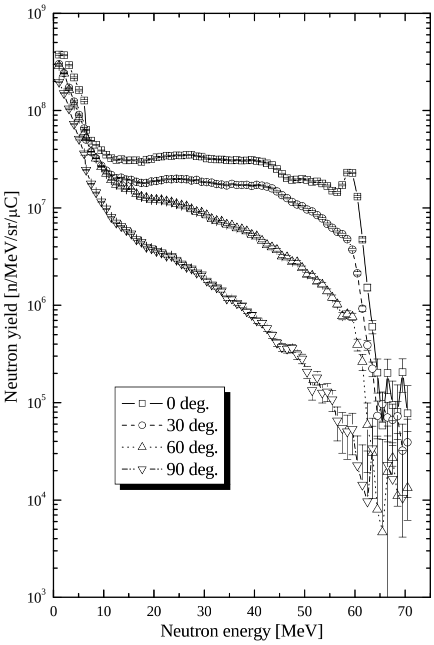

Fig. 3. ^{nat}Fe(p, xn) neutron production cross section

5. Results and discussion

5.1 Experimental data

Figures 2 and 3 show the preliminary results of differential neutron production cross section for the ^{nat}C and ^{nat}Fe(p,xn) reactions at 70 MeV. The data should be confirmed for the absolute value.

In the C(p,n) spectrum shown in fig. 2, a sharp edges exist around 52 MeV due to the ^{12}C(p,n) process which is the main components of the reaction with the Q-value of -18.1 MeV. On the other hand, there is also high energy component emitted from the ^{13}C(p,n) process with the Q-value of -3.0 MeV from ^{13}C whose natural content is about 1.1 % , The spectra show very strong angular dependence and energy-angle correlation because of light mass of C. .

In the case of iron, as shown in fig. 3, the spectrum shows no marked structures. The neutron spectra show pronounced increase in lowest energy region because of evaporation neutrons with the yields larger than light nuclides like ^{nat}C. The angular dependence of the spectra becomes stronger with increasing neutron energy.

5.2 Comparison with LA150

In this section, experimental TTY data are compared with the LA150 evaluated proton and neutron data libraries through the calculation by MCNPX [6] ver. 2.5e to take account of finite geometry and angular effects [7-8]. Figures 4 and 5 show the comparisons of our TTY experimental data and the calculations for ^{nat}C, ^{nat}Fe(p, xn) reactions.

In the case of ^{nat}C(p, xn) reaction, two components (^{12}C, ^{13}C(p, xn)) are visible similarly with the production cross sections, but the spectrum is generally much softer than the cross section itself. LA150 overestimates the experimental data in higher energy region and underestimates the energy region above around 50 MeV because LA150 lacks the contribution of ^{13}C. In the case of ^{nat}Fe(p, xn) reaction, the calculation reproduces the experimental data fairly well expect for those at backward angles.

Figure 6 and 7 show the comparisons of the present cross section data with the calculations. The calculations are normalized to the experimental data at 20 MeV. For ^{nat}C(p, xn) reaction, LA150 underestimates experimental data in higher energy region similarly with the case of thick target. For ^{nat}Fe(p, xn) reaction, LA150 reproduce experimental data generally well.

6. Conclusion and future plan

In this study, we measured the energy and angular double differential neutron emission cross sections for carbon and iron targets bombarded by 70 MeV protons using the CYRIC AVF cyclotron, Tohoku University. The data were obtained for neutron energy range down to 0.6 MeV and 0, 30, 60 and 90 deg.

The measured data were compared with calculations using MCNPX with LA150 data liberally. From these comparisons and past experimental data, LA150 reproduce generally well the experimental data while there is a room for improvement for high energy region.

We have plan to measure thin target neutron yields for Al, Cu, Ta and Pb(p, xn) reactions. In addition, we will upgrade the method of proton counting for the measurements of absolute neutron yield.

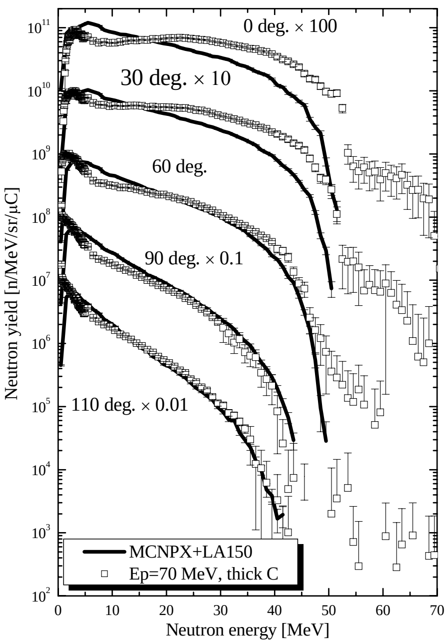

Fig. 4. Thick ^{nat}C(p, xn)

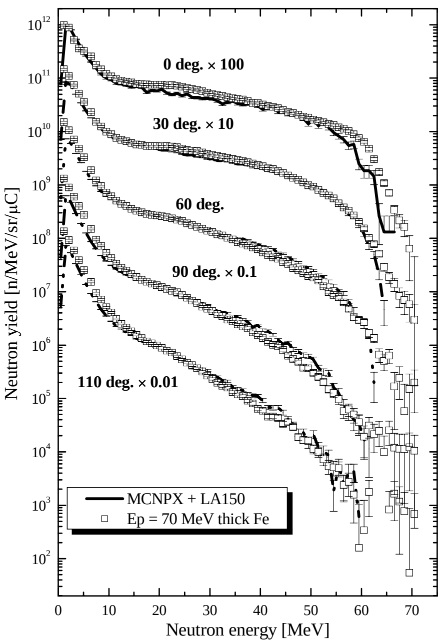

Fig. 5. Thick ^{nat}Fe(p, xn)

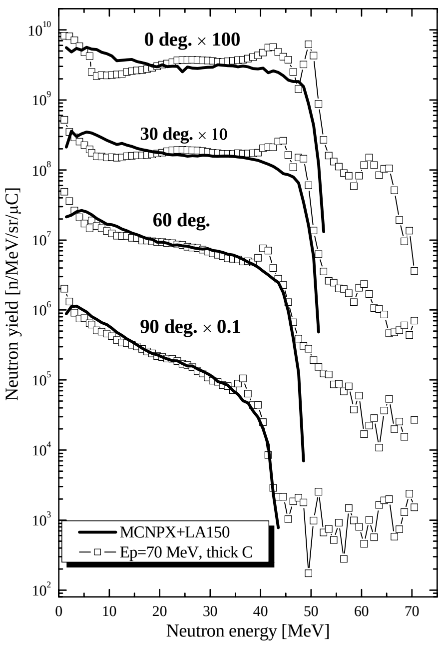

Fig. 6. ^{nat}C(p, xn)

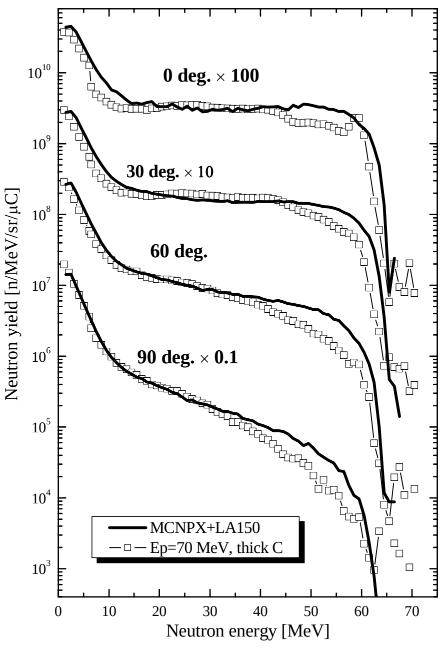

Fig. 7. ^{nat}Fe(p, xn)

References

[1] T. Aoki, M. Baba, S. Yonai, *et al.*, “Measurement of Differential Thick-Target Neutron Yields of C, Al, Ta, W(p, xn) Reactions for 50-MeV Protons”, *Nucl. Sci. Eng.*, **146**, 200, 2004.

[2] A. Terakawa, H. Suzuki, K. Kumagai, *et al.*, “New fast-neutron time-of-flight facilities at CYRIC”, *Nucl. Instr. and Meth.*, **491**, 419, 2002.

[3] M. Ibaraki, M. Baba, S. Matsuyama, *et al.*, “Measurement of Double-differential Neutron Emission Cross Section of ^{6}Li, ^{7}Li and ^{9}Be for 11.5 MeV and 18.0 MeV Neutrons”, *J. Nucl. Sci. Technol.*, **35** [12], 843, 1998.

[4] J. K. Dickens. ORNL-6463. Oak Ridge National Laboratory, 1988.

[5] S. Meigo. “Measurements of the responce function and the detection efficiency of an NE213 scintillator for neutrons between 20 and 65 MeV”, *Nucl. Instr. and Meth. in Phys. Res. A*, **401**, 365, 1997.

[6] L. S. Waters (Ed.), “MCNPX User’s Manual version 2.5.e”, LA-UR-04-0569, Los Alamos National Labolatory, 2004.

[7] M. B. Chadwick, P. G. Young, R. E. MacFarlane, *et al.*, “LA150 Documentation of Cross Sections, Heating, and Damage: Part A (Incident Neutrons)”, LANL Accelerator Production of Tritium Program, 1999.

[8] M. B. Chadwick, P. G. Young, R. E. MacFarlane, et al., “LA150 Documentation of Cross Sections, Heating, and Damage: Part B (Incident Protons)”, LANL Accelerator Production of Tritium Program, 1999.